

## Research Article

# Carbon Dot Functionalized Papers for the Selective Detection of 2,4,6-Trinitrophenol in Aqueous Solutions

Wenli Peng, Li Gan, Weihan Li, and Shixiong Deng 

Laboratory of Forensic Medicine & Biomedical Informatics, Chongqing Medical University, #1 Yixueyuan Road, Chongqing 400016, China

Correspondence should be addressed to Shixiong Deng; dengshixiong1963@163.com

Received 4 August 2021; Revised 31 August 2021; Accepted 1 September 2021; Published 17 September 2021

Academic Editor: Wei Liu

Copyright © 2021 Wenli Peng et al. This is an open access article distributed under the Creative Commons Attribution License, which permits unrestricted use, distribution, and reproduction in any medium, provided the original work is properly cited.

The development of probes for the testing of the carcinogenic pollutant 2,4,6-trinitrophenol (TNP) is of great importance for environmental protection and human health. In this paper, a new rapid and sensitive fluorescence detection method based on carbon dots (CDs) was designed for the detection of TNP. The CDs were synthesized by simple pyrolysis using citric acid as raw material and characterized by various advanced techniques. The addition of TNP caused a significant turn off in the fluorescence of the CDs. The fluorescence quench intensity and TNP concentration exhibited a good linear correlation in the range of 0–80  $\mu\text{M}$  with a minimum detection limit of 0.48  $\mu\text{M}$  and a related coefficient of 0.994. The analytical method was applied to the determination of trace TNP in river water and tap water with recoveries in the range of 98%–110% and relative standard deviations less than 5%. Importantly, carbon dots functionalized papers (CDFPs) were prepared using the synthesized CDs and successfully applied to the determination of TNP in aqueous solutions, demonstrating the promising application of the method.

## 1. Introduction

2,4,6-Trinitrophenol (TNP) is a nitroaromatic compound that is widely used in the preparation of military explosives, pharmaceuticals, matches, insecticides, leather, glass, dyes, and fireworks [1–3]. Due to its high explosive velocity and low safety factor, TNP has more intense explosive properties than the well-known TNT [4, 5]. In addition, its widespread use in several industries has led to soil and water contamination due to its high water solubility [6–9]. Furthermore, TNP is also a highly carcinogenic agent with hepatic and renal toxicity [10–12]. Once TNP enters the body, it can cause damage to the eyes, skin, respiratory system, nervous system, liver, and kidneys and even induce a series of health problems such as anemia, cyanosis, male infertility, and cancer [13–17]. Given the impact of TNP on human health, the surrounding environment, and social and public safety issues, there is an urgent need to establish a rapid and sensitive method that can be used for on-site trace TNP detection. So far, many methods applied to TNP detection such as electrochemistry [18], mass spectrometry [19],

surface-enhanced Raman spectroscopy [20], and colorimetric methods [21] have been able to meet market demand, but their application is limited by time-consuming, pretreatment processes, expensive instruments, complex operations, and low sensitivity and selectivity. In contrast, fluorescence-based detection methods are of interest because of their simplicity of operation, sensitivity, and low cost [22–25]. The common fluorescence analysis methods for TNP detection are mainly based on metal nanoclusters [26], photoluminescent polymers [27], organic frameworks [28–30], and semiconductor quantum dots doped with heavy metals [31, 32], which have low stability and environmental pollution problems. Therefore, a new fluorescent material that overcomes these limitations is needed for the rapid and sensitive detection of TNP.

Currently, carbon dots (CDs), as a novel nanomaterial, have been extensively applied in bioimaging, chemical sensors, drug delivery, and photocatalysis due to their outstanding water solubility, biocompatibility, low toxicity, and ease of synthesis [33–35]. In this study, we prepared fluorescent CDs by a simple hydrothermal route using

citric acid as a precursor. The synthesis process is shown in Scheme 1. After the addition of TNP, the fluorescence of CDs was apparently quenched because of the internal filter effect (IFE). Therefore, the detection of TNP was achieved by the fluorescence quench of synthetic CDs. In addition, the effects of pH, ionic strength, incubation time, nitro analogs, and common metal ions on the fluorescence intensity of the synthesized CDs were discussed. Using the optimized parameters, the prepared fluorescent probes were validated and succeeded in the application for the detection of TNP in tap and river water. Importantly, the carbon dot functionalized papers prepared using CDs as probes showed good selectivity and sensitivity for trace amounts of TNP in water samples, demonstrating their remarkable potential for real-time and in situ detection of environmental pollutants.

## 2. Experiments

**2.1. Materials.** 2,4,6-Trinitrophenol (TNP) was purchased from Beijing Zhongke Yingchuang Biotechnology Co. p-Nitrophenol (NP), p-nitrochlorobenzene (NC), nitrobenzene (NB), 1-chloro-2,4-dinitrobenzene (CDNB), and 1,3-dinitrobenzene (DNB) were purchased from Aladdin Co. Water samples were taken from tap water and Jialing River. All chemicals were of analytical grade and utilized directly without further purification.

**2.2. Characterization.** The morphological profile and particle size distribution of the CDs were assessed using an FEI Tecnai G2 F20 transmission electron microscope (TEM). Diffraction patterns of the CDs were recorded with an X-ray diffractometer (XRD) (X'Pert PRO MPD) at an accelerating voltage of 40 kV. The chemical composition of the CDs was obtained by X-ray photoelectron spectroscopy (XPS) (Thermo ESCALAB 250XI) analysis. Fourier transform infrared (FT-IR) spectroscopy was carried out using a Bruker Vertex 70 spectrometer at 4000–500  $\text{cm}^{-1}$ . Fluorescence experiments on the prepared fluorescent CDs and mixtures of CDs with TNP were recorded on an FS5 fluorescence spectrophotometer in the wavelength range 300–600 nm. UV-Vis absorption spectra were recorded on a UV-2600 UV spectrophotometer in the wavelength range 200–600 nm. Absolute fluorescence quantum yields were determined on an Edinburgh FLS9800 (steady-state transient spectrometer). The CDs and CDs-TNP complexes were evaluated using a fluorescence lifetime system.

**2.3. Preparation of CDs.** 1.0507 g of citric acid was added to 10 mL of deionized water. The mixed solution was then transferred to an autoclave (30 mL) lined with Teflon and heated for 5 hours at 200°C. It was cooled to room temperature, filtered through a microporous filter (0.45  $\mu\text{M}$ ), and purified using a dialysis bag (MWCO = 3500) for 24 h. Finally, the resulting solution was freeze-dried under a vacuum to obtain the purified CDs.

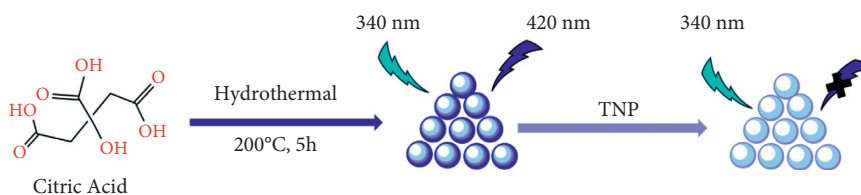
**2.4. Detection of TNP.** A mixture of CDs and TNP was obtained by mixing 1 ml of CDs solution (0.2 mg/ml) with 1 ml of different concentrations of TNP (0, 1, 2, 10, 20, 40, 60, and 80  $\mu\text{M}$ ). The solution was kept at room temperature with shaking for 3 min. The fluorescence quenching effect of CDs was observed with a fluorescence spectrometer under 340 nm excitation.

**2.5. Sample Pretreatment.** Tap water and river water samples were taken locally from Chongqing. Water samples were centrifuged and filtered through 0.45  $\mu\text{M}$  microporous filters.

**2.6. Preparation of CDFPs.** The CDFPs were prepared as described in the previous literature [36]. In brief, a wax printer was used to print a circular hole pattern on one side and wax on the other side of the chromatography paper. The wax-imprinted chromatography paper was put on a heating table and heated at 150°C for 1 min to melt the wax to form a hydrophobic layer. The prepared carbon dot solution (4  $\mu\text{l}$ ) was placed in each circular hole of the wax-printed paper. The excess solvent was evaporated in an oven at 50°C.

## 3. Results and Discussion

**3.1. Synthesis and Characterization of CDs.** The XRD diffraction pattern (Figure 1(a)) shows a broad peak located at  $2\theta = 24.1^\circ$ , comparable to the graphite lattice spacing (002), which is consistent with previous reports, and confirms that the synthesized CDs have a similar graphene structure [37]. The morphology and dimensions of the prepared CDs were characterized by TEM, as shown in Figure 1(b). The synthesized CDs are subspherical in shape and have good dispersion in aqueous solution. Figure 1(c) shows the lattice spacing of the prepared CDs. The particle size distribution of the CDs (Figure 1(d)) shows a narrow range of diameters from 1.49 to 3.09 nm, with an average diameter of 2.2 nm. We then investigated the optical properties of the synthesized fluorescent CDs using fluorescence spectroscopy and UV absorption spectroscopy. As shown in Figure 2(a), CDs do not have a prominent absorption peak in the visible region, but there is significant absorption at 200–300 nm. The fluorescence emission spectra of CDs were obtained at 10 nm intervals at different excitation wavelengths in the range of 310–400 nm. As shown in Figure 2(b), the fluorescence spectrum is red-shifted with increasing excitation wavelength. The carbon dot shift between the emission and excitation wavelengths is 80 nm, indicating that the synthesized CDs could be used as a candidate analytical material. The fluorescence quantum yield, an important property of synthetic CDs, is calculated to be 5.9%, which is comparable to the previously reported yield of undoped quantum dots [38]. The chemical bonding and functional groups at the carbon sites were further investigated using FT-IR spectroscopy (Figure 3(a)). The broad and strong peak at 3490  $\text{cm}^{-1}$  is attributed to the –OH stretching vibration [39]. The vibrational peak at 1724  $\text{cm}^{-1}$  is thought to be the C=O stretching vibration [40]. The stretching peak at



SCHEME 1: Synthesis of fluorescent CDs and detection of TNP.

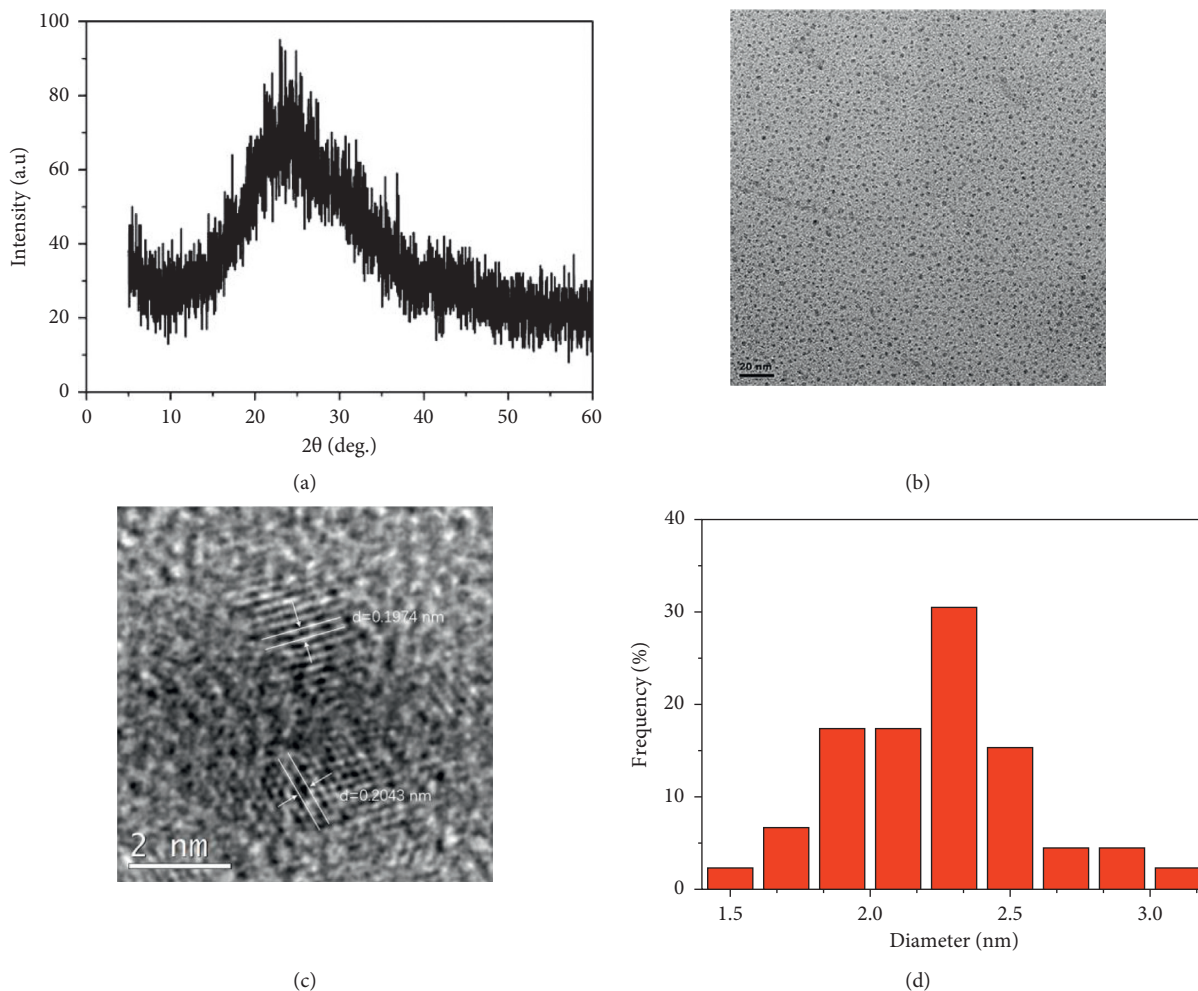


FIGURE 1: (a) XRD of CDs, TEM image (b), HR-TEM and lattice fringes image (c), and the size distribution (d) of CDs.

$1187\text{ cm}^{-1}$  is attributed to C-O [41]. The bands at  $920\text{ cm}^{-1}$  and  $780\text{ cm}^{-1}$  are identified as out-of-plane bending vibrations of the O-H bond. To further investigate the elemental composition of the CDs, they were subjected to further XPS assays. As shown in Figure 3(b), the wide scan XPS spectrum shows two peaks centered at 285.3 eV and 533.2 eV, attributed to the C 1s and O 1s signals, respectively [42]. The C 1s (Figure 3(c)) show three peaks, which correspond to C-C (284.8 eV), C-O (286.6 eV), and O=C-O (288.8 eV), respectively [43]. The O 1s peak (Figure 3(d)) can be deconvoluted into two peaks, C-O (531.7 eV) and O-C=O (532.9 eV) [44]. The peaks associated with the hydroxyl and carboxyl functional groups in the XPS analysis results are consistent with the FT-IR spectra of the CDs, favoring

solubility and stability in water. The above results indicate that the blue fluorescent probes are successfully synthesized and can be further analyzed for applications.

**3.2. Parameter Optimization.** Various factors such as buffer pH, ionic strength, and incubation time can affect the fluorescence intensity of CDs, so a series of experiments were carried out to optimize the parameters for the analysis of CDs. Firstly, the influence of PH on the fluorescence of CDs was studied, and the findings are illustrated in Figure 4(a). The fluorescence intensity of CDs remained relatively stable at pH 7.0–9.0. Therefore, we chose the pH 7.0 buffer for the sensitive detection of TNP. The effect of ion

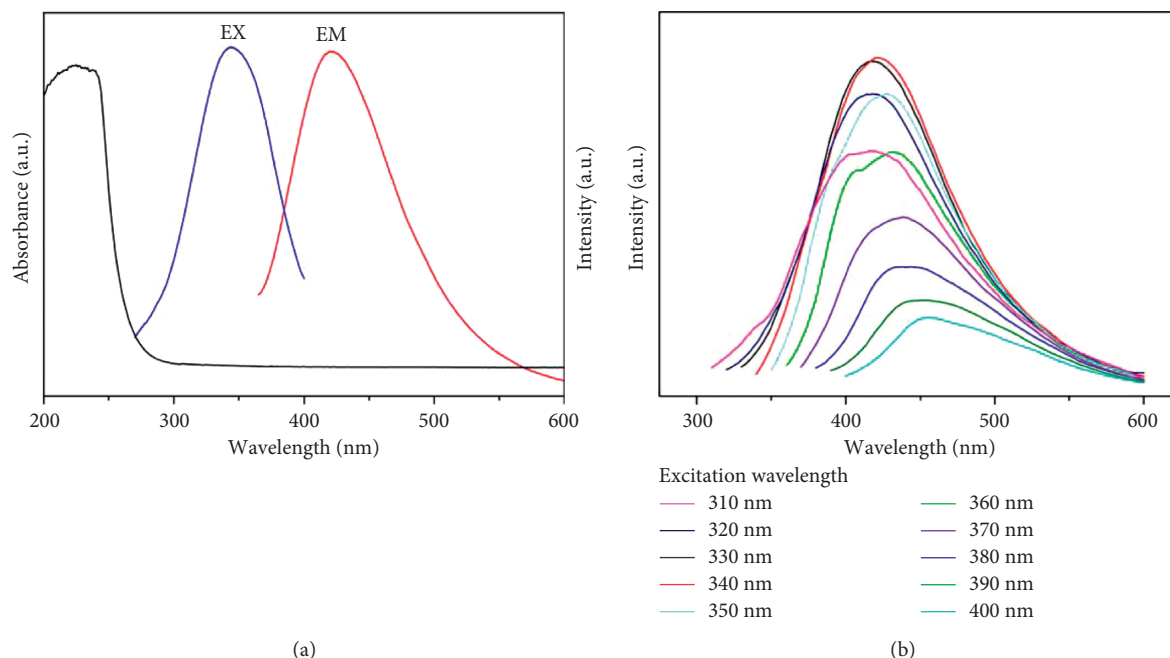


FIGURE 2: (a) UV absorption spectra and fluorescence excitation (Ex) and emission (Em) spectroscopy. (b) Fluorescence spectra of CDs at different excitation wavelengths.

concentration was then explored, as shown in Figure 4(b). The fluorescence intensity remained essentially constant at different concentrations of NaCl solution, which demonstrates that CDs can be detected at stronger ionic concentrations. In addition, the relationship between incubation time and carbon dot fluorescence was investigated to ascertain the altered kinetics of the probes. As shown in Figure 4(c), the fluorescence of the CDs was effectively burst during 7 minutes after the incorporation of  $20\ \mu\text{M}$  TNP, indicating that the 7-minute incubation time could be used for further analytical studies. Therefore, we chose a pH 7.0 buffer incubated for 7 minutes at room temperature for the sensitive detection of TNP.

**3.3. Analysis of Performance.** The above optimized analytical parameters were adopted to detect different concentrations of TNP and to evaluate the analysis properties of the presented fluorescent probes. Figure 5(a) shows the fluorescence spectra of the fluorescent CDs at 340 nm excitation under the effect of different levels of TNP. It can be seen that the fluorescence of the CDs is gradually quenched as the concentration of TNP increased. We plotted the Stern–Volmer curve between  $\log(I_0/I)$  and TNP (Figure 5(b)), where  $I_0$  and  $I$  represent the fluorescence intensity of CDs in the absence and presence of TNP. It showed a good linear relationship between the burst of fluorescence and TNP concentration in the  $0\text{--}80\ \mu\text{M}$  range with a regression coefficient ( $R^2$ ) of 0.994. The regression equation is  $\log(I_0/I) = 0.007c\ (\mu\text{M}) - 0.014$ . The limit of detection (LOD) was  $0.48\ \mu\text{M}$  ( $3\sigma/k$ ,  $n = 3$ ), which was calculated from the standard deviation (SD) of the response and the slope of the calibration curve (S), which is

comparable to previous studies (Table 1) in the literature. As the concentration of TNP increased, the bright blue fluorescence of the CDs-TNP mixture was gradually quenched under the UV lamp, while a change in colour could be seen in the CDs-TNP mixture, visually demonstrating the quenching phenomenon (Figure 5(c)). Therefore, our proposed analytical method has high affinity and sensitivity for the detection of trace amounts of TNP.

**3.4. Study of Possible Mechanisms.** To investigate the mechanism of quenching of the prepared fluorescent probes, we investigated the optical properties of CDs and CDs-TNP complexes. In the recently published literature, three common mechanisms of fluorescence quenching include fluorescence resonance energy transfer, photoinduced electron transfer, and fluorescence internal filtration [45]. As shown in Figure 6(a), the emission spectra of CDs clearly superimpose on the absorbance spectrum of TNP, suggesting that the fluorescence quenching mechanism may be IFE or FRET [46]. As shown in Figure 6(b), the addition of TNP ( $20\ \mu\text{M}$ ) changed the fluorescence lifetime from 2.222 ns to 2.198 ns, which showed little change in fluorescence lifetime, in agreement with previous reports [47], ruling out the possibility of a quenching mechanism for FRET and PET [48]. Therefore, the fluorescence quenching mechanism of CDs was attributed to the IFE between TNP and CDs.

**3.5. Selective Detection.** An important factor in the evaluation of the prepared fluorescent probes is selectivity. It was possible to detect the selectivity of the proposed fluorescent probes by assessing the change in the fluorescence intensity

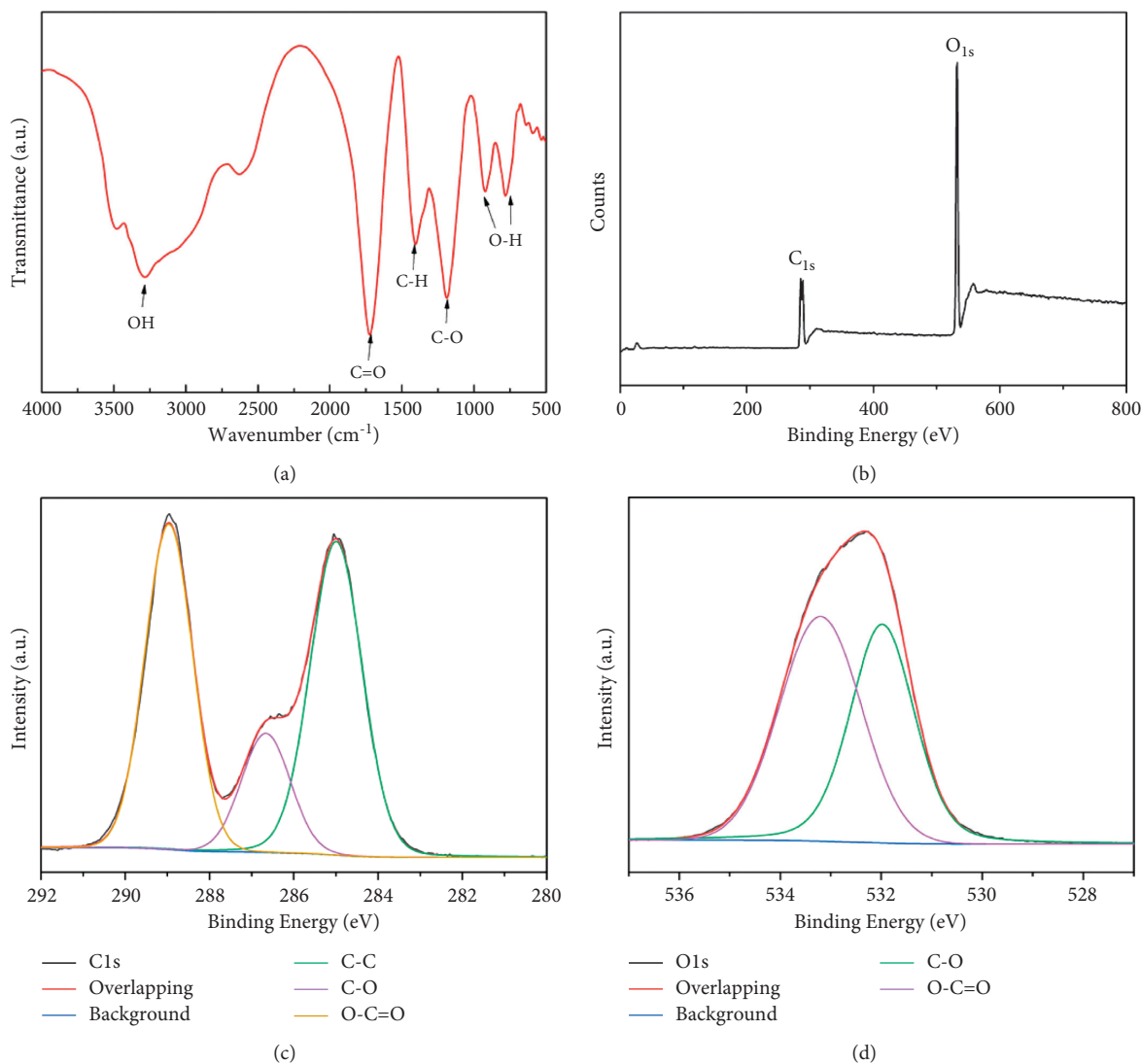


FIGURE 3: (a) FT-IR spectra of the CDs. (b) XPS survey of CDs. The high resolution of C 1s (c) and O 1s (d) spectra of the CDs.

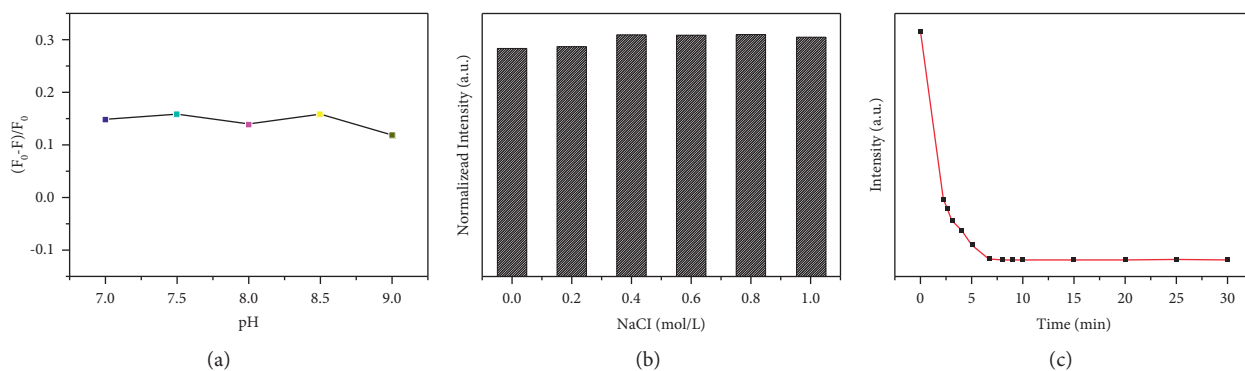


FIGURE 4: (a) Fluorescence quenching efficiency at different pH values. Normalized fluorescence intensity of CDs added to TNP at different NaCl concentrations (b) and incubation periods (c).

of the prepared CDs in the presence of TNP and other similar nitroaromatic compounds (NP, NC, NB, and CDNB). As shown in Figure 7(a), the fluorescence intensity

of the CDs was significantly quenched by the addition of TNP compared to the other nitro compounds, showing the good selectivity of the prepared fluorescent probes for TNP.

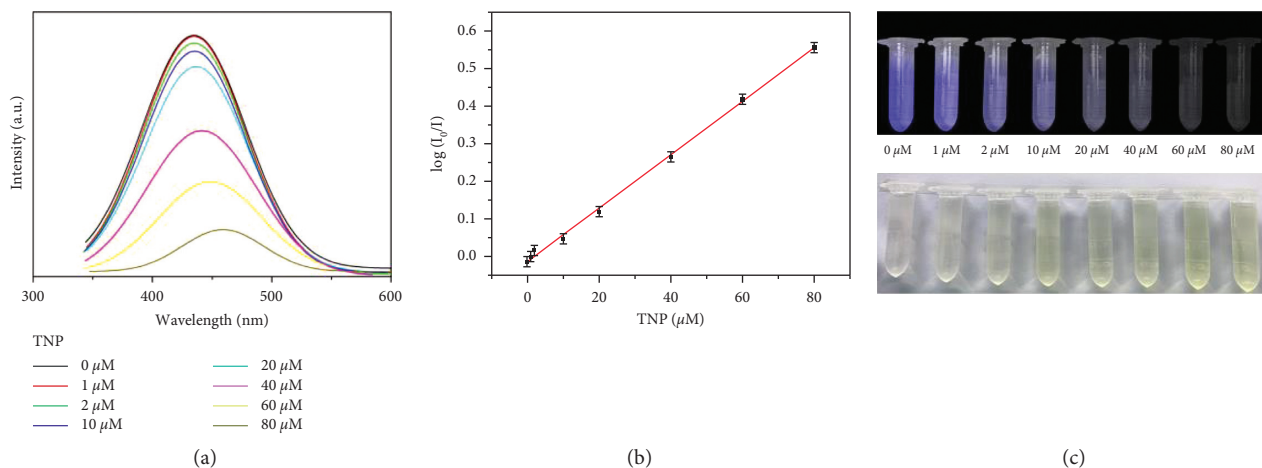


FIGURE 5: (a) Fluorescence emission spectra of CDs added with different concentrations of TNP. (b) Relationship between relative fluorescence intensity ( $\log I_0/I$ ) ( $I_0$  and  $I$  represent the fluorescence intensity of CDs in the absence and presence of TNP, respectively) and different concentrations of TNP. (c) Changes in fluorescence under UV light and visible to the naked eye after the addition of different concentrations of TNP.

TABLE 1: Comparison of different methods for the determination of TNP.

Material	Linear range ( $\mu\text{M}$ )	LOD ( $\mu\text{M}$ )	Reference
CQDs	1–110	1.8	[49]
N-GQDs	1–60	0.3	[50]
BNQDs	0.25–100	0.14	[51]
CDs	0–100	0.02	[52]
CDs	0.5–200	0.2	[53]
CNPs	0.5–100	0.25	[54]
CDs	0–80	0.48	Present work

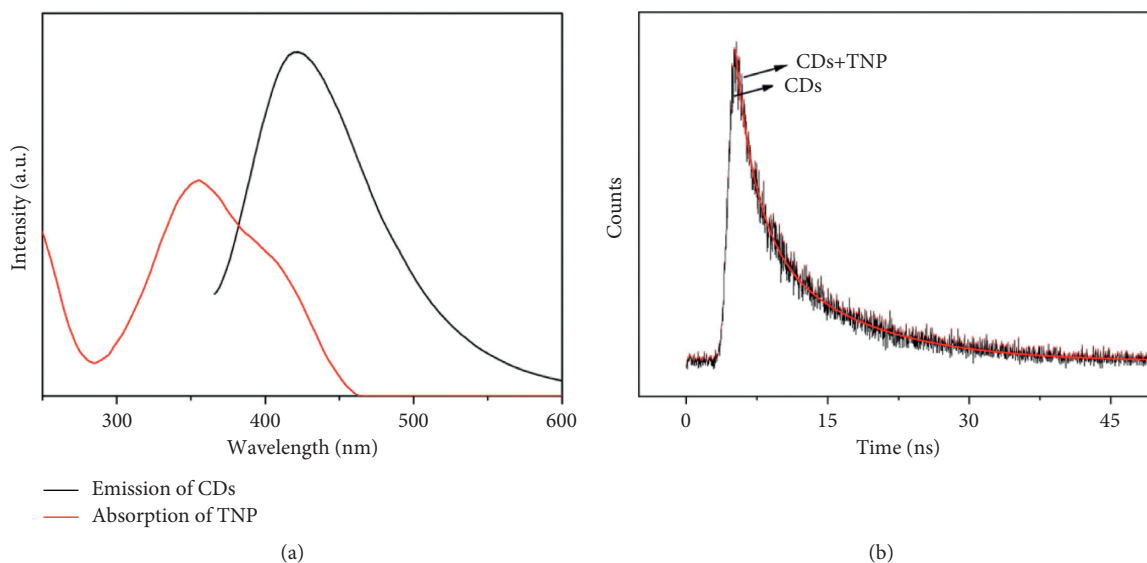


FIGURE 6: (a) The UV absorption spectrum of TNP and fluorescence spectrum of CDs. (b) The fluorescence lifetime and fitting curve of CDs.

The selective detection of TNP was also applied to common metal ions. The results are shown in Figure 7(b). The effect of metal ions is almost negligible compared to TNP, indicating that the prepared probes still have good selectivity despite the interference of metal ions.

**3.6. Assaying TNP in Real Aqueous Samples.** To test the practical application of the prepared probes, the prepared CDs were used to detect TNP in actual samples. We collected Jialing River water and tap water locally in Chongqing, and after adding different concentrations of TNP, the recoveries

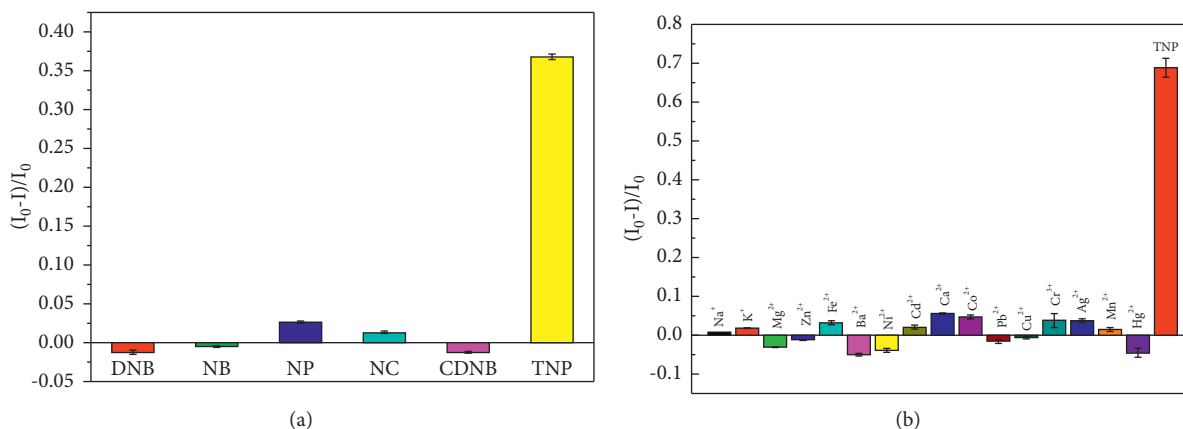


FIGURE 7: (a, b) The efficiency of fluorescence quenching of CDs in the presence of different analytes.  $I_0$  and  $I$  represent the fluorescence intensity of CDs in the absence and presence of different analytes, respectively.

TABLE 2: Results of the recovery analysis of TNP in water samples.

Samples	Added ( $\mu\text{mol/L}$ )	Founded ( $\mu\text{mol/L}$ )	Recovery (%)	RSD ( $n = 3$ ) (%)
Tap water	0.5	0.53	106	2.8
	1	1.03	103	2.7
	2	2.2	110	3.4
River water	0.5	0.49	98	2.8
	1	1.01	101	3.2
	2	2.04	102	2.6

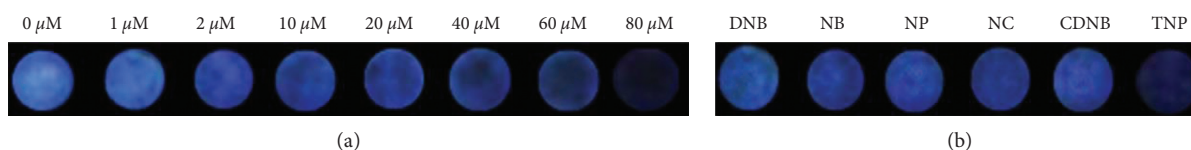


FIGURE 8: Sensitivity (a) and selectivity (b) of CDFPs to TNP detection.

were analyzed and the findings are demonstrated in Table 2, where the recoveries of the samples ranged from 98% to 110% with relative standard deviations of less than 5% for each sample for three experiments. The analytical method proved to have good accuracy and recovery. Therefore, the sensor can be implemented for the detection of real samples.

**3.7. Detection of TNP by CDFPs.** To demonstrate the rapid sensitivity and easy portability of CDs for TNP detection, the CDFPs were prepared by immersing filter paper in solutions of different concentrations of CDs and drying at room temperature. It was found that the functionalized paper immobilised with  $400 \mu\text{g/mL}$  CDs showed the strongest fluorescence under UV light. Therefore, a carbon dot concentration of  $400 \mu\text{g/mL}$  was chosen as the optimum concentration for the preparation of CDFPs. The functionalized paper immobilised with  $400 \mu\text{g/mL}$  CDs was treated with different concentrations of TNP, as shown in Figure 8(a). The fluorescence intensity of the indicator paper gradually decreased as the TNP concentration increased from 0 to

$80 \mu\text{M}$ , indicating a rapid and naked-eye sensitive detection of TNP. Because of the relatively low emission backdrop of the chromatography paper, we chose a portable laser lamp at 254 nm, although the photoluminescence of the CDs was stronger at 360 nm excitation. In addition, we examined common nitro analogs using the prepared carbon dot functionalized paper. The results are shown in Figure 8(b), where the fluorescence quench of TNP on CDs is visible to the naked eye under UV lamp irradiation, demonstrating its potential application in the field for the detection of TNP.

## 4. Conclusion

In summary, we synthesized environmentally friendly CDs using citric acid as the precursor. The prepared CDs showed excitation-dependent behavior at 310 nm–400 nm with a fluorescence QY of 5.9%. The results show that the synthesized CDs can be used as detection probes for TNP with high selectivity and sensitivity in the range of 0– $80 \mu\text{M}$  TNP concentration and a detection limit of  $0.48 \mu\text{M}$ . More

importantly, the CDFPs we prepared were effectively used in actual water samples, showing promising potential for field monitoring of environmental water samples.

### Data Availability

The data that support the findings of this study are available from the corresponding author upon reasonable request.

### Conflicts of Interest

The authors declare no conflicts of interest.

### Authors' Contributions

Li Gan and Weihan Li helped to revise manuscript. Shixiong Deng revised the manuscript and coordinated the study.

### Acknowledgments

This study was supported by funding from the Basic Medicine College, Chongqing Medical University. The authors are grateful for the financial support of this study.

### References

- [1] S. Lu, M. Xue, A. Tao et al., "Facile microwave-assisted synthesis of functionalized carbon nitride quantum dots as fluorescence probe for fast and highly selective detection of 2,4,6-trinitrophenol," *Journal of Fluorescence*, vol. 31, no. 1, pp. 1-9, 2021.
- [2] S. Kumar, N. Venkatramaiah, and S. Patil, "Fluoranthene based derivatives for detection of trace explosive nitroaromatics," *Journal of Physical Chemistry C*, vol. 117, no. 14, pp. 7236-7245, 2013.
- [3] N. Li, S. G. Liu, Y. Z. Fan et al., "Adenosine-derived doped carbon dots: from an insight into effect of N/P co-doping on emission to highly sensitive picric acid sensing," *Analytica Chimica Acta*, vol. 1013, pp. 63-70, 2018.
- [4] Y. J. Ju, N. Li, S. G. Liu et al., "Green synthesis of blue fluorescent P-doped carbon dots for the selective determination of picric acid in an aqueous medium," *Analytical Sciences*, vol. 35, no. 2, pp. 147-152, 2019.
- [5] J. H. Liu, F. F. Wu, A. Xie, C. F. Liu, and H. J. Bao, "Preparation of nonconjugated fluorescent polymer nanoparticles for use as a fluorescent probe for detection of 2,4,6-trinitrophenol," *Analytical and Bioanalytical Chemistry*, vol. 412, no. 5, pp. 1235-1242, 2020.
- [6] J. Wang, Y. Yang, G. Sun, M. Zheng, and Z. Xie, "A convenient and universal platform for sensing environmental nitro-aromatic explosives based on amphiphilic carbon dots," *Environmental Research*, vol. 177, Article ID 108621, 2019.
- [7] V. Srinivasan, M. Asha Jhonsi, M. Kathiresan, and A. Kathiravan, "Nanostructured graphene oxide dots: synthesis, characterization, photoinduced electron transfer studies, and detection of explosives/biomolecules," *ACS Omega*, vol. 3, no. 8, pp. 9096-9104, 2018.
- [8] J. Li, N. Zhang, Y. Yuan et al., "A luminescent Cd(II)-metal organic frameworks combined of TPT and H3BTC detecting 2,4,6-trinitrophenol and chromate anions in aqueous," *Spectrochimica Acta Part A: Molecular and Biomolecular Spectroscopy*, vol. 242, Article ID 118790, 2020.
- [9] K. C. Remani and N. N. Binitha, "Fluorescence sensing of picric acid by ceria nanostructures prepared using fenugreek extract," *Journal of the Iranian Chemical Society*, 2021.
- [10] Y. Meng, Y. Jiao, Y. Zhang et al., "Multi-sensing function integrated nitrogen-doped fluorescent carbon dots as the platform toward multi-mode detection and bioimaging," *Talanta*, vol. 210, Article ID 120653, 2020.
- [11] M. Tian, Y. Wang, and Y. Zhang, "Synthesis of fluorescent nitrogen-doped carbon quantum dots for selective detection of picric acid in water samples," *Journal of Nanoscience and Nanotechnology*, vol. 18, no. 12, pp. 8111-8117, 2018.
- [12] Y. Zheng, S. Wang, R. Li, L. Pan, L. Li, and Z. Qi, "Highly selective detection of nitroaromatic explosive 2,4,6-trinitrophenol (TNP) using N-doped carbon dots," *Research on Chemical Intermediates*, vol. 47, no. 6, pp. 2421-2431, 2021.
- [13] B. Chen, S. Chai, J. Liu et al., "2,4,6-Trinitrophenol detection by a new portable sensing gadget using carbon dots as a fluorescent probe," *Analytical and Bioanalytical Chemistry*, vol. 411, no. 11, pp. 2291-2300, 2019.
- [14] X. Wang, X. Zhang, H. Cao, and Y. Huang, "A facile and rapid approach to synthesize uric acid-capped Ti3C2 MXene quantum dots for the sensitive determination of 2,4,6-trinitrophenol both on surfaces and in solution," *Journal of Materials Chemistry B*, vol. 8, no. 47, pp. 10837-10844, 2020.
- [15] Y. L. Wang, Y. L. Wan, Y. P. Zhou, Y. H. Li, and C. P. Liu, "A luminescent Zn(II)-Organic framework: selective sensing of 2,4,6-trinitrophenol and curing importance combined with ginsenoside on sepsis mice," *Journal of Cluster Science*, 2021.
- [16] R. R. Gao, J. H. Wang, H. Wang, W. Dong, and J. W. Zhu, "Fluorescent nucleotide-lanthanide nanoparticles for highly selective determination of picric acid," *Microchimica Acta*, vol. 188, no. 1, p. 18, 2021.
- [17] J. Liu, T. Fu, C. Liu, F. Wu, and H. Wang, "Sensitive detection of picric acid in an aqueous solution using fluorescent nonconjugated polymer dots as fluorescent probes," *Nanotechnology*, vol. 32, no. 35, Article ID 355503, 2021.
- [18] J. Z. Wei, X. L. Wang, X. J. Sun et al., "Rapid and large-scale synthesis of IRMOF-3 by electrochemistry method with enhanced fluorescence detection performance for TNP," *Inorganic Chemistry*, vol. 57, no. 7, pp. 3818-3824, 2018.
- [19] Y. Liu, T. L. Zhang, L. Yang, B. D. Wu, and R. Liu, "QuEChERS-ultra performance liquid chromatography-tandem mass spectrometry for determination of 2,4,6-trinitrophenol, 2,4,6-trinitroresorcinol and 2,4,6-trinitrophenol in soil," *Chinese Journal of Analytical Chemistry*, vol. 42, no. 8, pp. 1183-1188, 2014.
- [20] V. Sivaprakasam and M. B. Hart, "Surface-enhanced Raman spectroscopy for environmental monitoring of aerosols," *ACS Omega*, vol. 6, no. 15, pp. 10150-10159, 2021.
- [21] Y. Peng, A. J. Zhang, M. Dong, and Y. W. Wang, "A colorimetric and fluorescent chemosensor for the detection of an explosive-2,4,6-trinitrophenol (TNP)," *Chemical Communications*, vol. 47, no. 15, pp. 4505-4507, 2011.
- [22] S. Dey, A. Maity, M. Shyamal et al., "An antipyrine based fluorescence "turn-on" dual sensor for Zn(2+) and Al(3+) and its selective fluorescence "turn-off" sensing towards 2,4,6-trinitrophenol (TNP) in the aggregated state," *Photochemical and Photobiological Sciences*, vol. 18, no. 11, pp. 2717-2729, 2019.
- [23] S. Xiong, L. Marin, L. Duan, and X. Cheng, "Fluorescent chitosan hydrogel for highly and selectively sensing of p-nitrophenol and 2, 4, 6-trinitrophenol," *Carbohydrate Polymers*, vol. 225, Article ID 115253, 2019.

- [24] S. Y. Zong, B. L. Wang, W. Y. Ma, Y. Yan, and J. Y. Li, "Carbon dots derived from coffee residue for sensitive and selective detection of picric acid and iron(III) ions," *Chemical Research in Chinese Universities*, vol. 37, no. 3, pp. 623–628, 2021.
- [25] J. Liu, H. Bao, C. Liu, F. Wu, and T. Fu, "Turn-on" fluorometric probe for hydroquinone and catechol based on an in situ reaction between protamine sulfate and dihydroxybenzene isomers and the formation of fluorescent polymer nanoparticles," *Sensors and Actuators B: Chemical*, vol. 333, Article ID 129565, 2021.
- [26] S. S. Ding, C. Y. Liu, D. Y. Fu, G. Y. Shi, and A. W. Zhu, "Coordination of ligand-protected metal nanoclusters and glass nanopipettes: conversion of a liquid-phase fluorometric assay into an enhanced nanopore analysis," *Analytical Chemistry*, vol. 93, no. 3, pp. 1779–1785, 2021.
- [27] M. Wang, M. J. Gao, L. L. Deng et al., "A sensitive and selective fluorescent sensor for 2,4,6-trinitrophenol detection based on the composite material of magnetic covalent organic frameworks, molecularly imprinted polymers and carbon dots," *Microchemical Journal*, vol. 154, Article ID 104590, 2020.
- [28] X. Zhang, Y. Yan, F. Q. Chen, G. X. Bai, H. Xu, and S. Q. Xu, "A fluorescent titanium-based metal-organic framework sensor for nitro-aromatics detection," *Zeitschrift für Anorganische und Allgemeine Chemie*, vol. 647, no. 7, pp. 759–763, 2021.
- [29] S. Z. Du, Z. Sun, L. Han, M. Qing, H. Q. Luo, and N. B. Li, "Two 3d-4f metal-organic frameworks as fluorescent sensor array for the discrimination of phosphates based on different response patterns," *Sensors and Actuators B: Chemical*, vol. 324, Article ID 128757, 2020.
- [30] X. C. Chen, F. Xi, R. Liu, and J. W. Zhou, "A Eu(III)-based metal organic framework: selective sensing of picric acid and nursing application values on the cerebral edema induced by cerebral hemorrhage via reducing the coagulation factor II activity," *Journal of Fluorescence*, vol. 31, no. 2, pp. 385–392, 2021.
- [31] M. Amjadi and R. Jalili, "Molecularly imprinted mesoporous silica embedded with carbon dots and semiconductor quantum dots as a ratiometric fluorescent sensor for diniconazole," *Biosensors and Bioelectronics*, vol. 96, pp. 121–126, 2017.
- [32] S. Liao, F. W. Zhu, X. Y. Zhao, H. Yang, and X. Q. Chen, "A reusable P, N-doped carbon quantum dot fluorescent sensor for cobalt ion," *Sensors and Actuators B: Chemical*, vol. 260, pp. 156–164, 2018.
- [33] F. F. Zhao, T. Y. Zhang, Y. Yang, and C. L. Lu, "A facile synthesis of multifunctional carbon dots as fluorescence "turn on" and "turn off" probes for selective detection of Al(3+) and 2,4,6-trinitrophenol," *Luminescence*, vol. 35, no. 8, pp. 1277–1285, 2020.
- [34] A. Kathiravan, A. Gowri, V. Srinivasan, T. A. Smith, M. Ashokkumar, and M. Asha Jhonsi, "A simple and ubiquitous device for picric acid detection in latent fingerprints using carbon dots," *Analyst*, vol. 145, no. 13, pp. 4532–4539, 2020.
- [35] Q. Ye, F. Yan, D. Shi et al., "N, B-doped carbon dots as a sensitive fluorescence probe for Hg(2+) ions and 2,4,6-trinitrophenol detection for bioimaging," *Journal of Photochemistry and Photobiology B*, vol. 162, pp. 1–13, 2016.
- [36] Y. T. Yen, Y. S. Lin, T. Y. Chen, S. C. Chyueh, and H. T. Chang, "Carbon dots functionalized papers for high-throughput sensing of 4-chloroethcathinone and its analogues in crime sites," *Royal Society Open Science*, vol. 6, no. 9, Article ID 191017, 2019.
- [37] L. Cai, Z. Fu, and F. Cui, "Synthesis of carbon dots and their application as turn off-on fluorescent sensor for mercury (II) and glutathione," *Journal of Fluorescence*, vol. 30, no. 1, pp. 11–20, 2020.
- [38] H. Li, X. He, Z. Kang et al., "Water-soluble fluorescent carbon quantum dots and photocatalyst design," *Angewandte Chemie International Edition in English*, vol. 49, no. 26, pp. 4430–4434, 2010.
- [39] J. Wei, J. Shen, X. Zhang et al., "Simple one-step synthesis of water-soluble fluorescent carbon dots derived from paper ash," *RSC Advances*, vol. 3, no. 32, Article ID 13119, 2013.
- [40] Y. Zhao, S. Zou, D. Huo et al., "Simple and sensitive fluorescence sensor for methotrexate detection based on the inner filter effect of N, S co-doped carbon quantum dots," *Analytica Chimica Acta*, vol. 1047, pp. 179–187, 2019.
- [41] J. Hou, W. Wang, T. Zhou, B. Wang, H. Li, and L. Ding, "Synthesis and formation mechanistic investigation of nitrogen-doped carbon dots with high quantum yields and yellowish-green fluorescence," *Nanoscale*, vol. 8, no. 21, pp. 11185–11193, 2016.
- [42] Y. Dong, H. Pang, H. B. Yang et al., "Carbon-based dots co-doped with nitrogen and sulfur for high quantum yield and excitation-independent emission," *Angewandte Chemie International Edition in English*, vol. 52, no. 30, pp. 7800–7804, 2013.
- [43] Z. Yang, M. Xu, Y. Liu et al., "Nitrogen-doped, carbon-rich, highly photoluminescent carbon dots from ammonium citrate," *Nanoscale*, vol. 6, no. 3, pp. 1890–1895, 2014.
- [44] X. Chen, Q. Jin, L. Wu, C. Tung, and X. Tang, "Synthesis and unique photoluminescence properties of nitrogen-rich quantum dots and their applications," *Angewandte Chemie International Edition in English*, vol. 53, no. 46, pp. 12542–12547, 2014.
- [45] Z. Liang, M. Kang, G. F. Payne, X. Wang, and R. Sun, "Probing energy and electron transfer mechanisms in fluorescence quenching of biomass carbon quantum dots," *ACS Applied Materials and Interfaces*, vol. 8, no. 27, pp. 17478–17488, 2016.
- [46] Y. Z. Fan, Y. Zhang, N. Li et al., "A facile synthesis of water-soluble carbon dots as a label-free fluorescent probe for rapid, selective and sensitive detection of picric acid," *Sensors and Actuators B: Chemical*, vol. 240, pp. 949–955, 2017.
- [47] Y. Ling, J. X. Li, F. Qu, N. B. Li, and H. Q. Luo, "Rapid fluorescence assay for Sudan dyes using polyethyleneimine-coated copper nanoclusters," *Microchimica Acta*, vol. 181, no. 9–10, pp. 1069–1075, 2014.
- [48] M. Rong, L. Lin, X. Song et al., "A label-free fluorescence sensing approach for selective and sensitive detection of 2,4,6-trinitrophenol (TNP) in aqueous solution using graphitic carbon nitride nanosheets," *Analytical Chemistry*, vol. 87, no. 2, pp. 1288–1296, 2015.
- [49] F. Cheng, X. An, C. Zheng, and S. Cao, "Green synthesis of fluorescent hydrophobic carbon quantum dots and their use for 2,4,6-trinitrophenol detection," *RSC Advances*, vol. 5, no. 113, pp. 93360–93363, 2015.
- [50] L. Lin, M. Rong, S. Lu et al., "A facile synthesis of highly luminescent nitrogen-doped graphene quantum dots for the detection of 2,4,6-trinitrophenol in aqueous solution," *Nanoscale*, vol. 7, no. 5, pp. 1872–1878, 2015.
- [51] D. Peng, L. Zhang, F. Li, W. R. Cui, and J. D. Qiu, "Facile and green approach to the synthesis of boron nitride quantum dots for 2,4,6-trinitrophenol sensing," *ACS Applied Materials & Interfaces*, vol. 10, no. 8, 2018.

- [52] X. Deng and D. Wu, "Highly sensitive photoluminescence energy transfer detection for 2,4,6-trinitrophenol using photoluminescent carbon nanodots," *RSC Advances*, vol. 4, no. 79, pp. 42066–42070, 2014.
- [53] A. B. Siddique, A. K. Pramanick, S. Chatterjee, and M. Ray, "Amorphous carbon dots and their remarkable ability to detect 2,4,6-trinitrophenol," *Entific Reports*, vol. 8, no. 1, p. 9770, 2018.
- [54] X. Sun, J. He, Y. Meng et al., "Microwave-assisted ultrafast and facile synthesis of fluorescent carbon nanoparticles from a single precursor: preparation, characterization and their application for the highly selective detection of explosive picric acid," *Journal of Materials Chemistry*, vol. 4, no. 11, pp. 4161–4171, 2016.